

A.V. Ryabykh¹, O.A. Maslova¹, S.A. Beznosyuk^{1*}, A.S. Masalimov²

¹Altai State University, Barnaul, Russia;

²Karagandy University of the name of academician E.A. Buketov, Karaganda, Kazakhstan

(*Corresponding author's e-mail: bsa1953@mail.ru)

The Role of Zinc Ion in the Active Site of Copper-Zinc Superoxide Dismutase

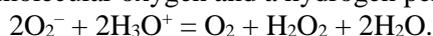
The interaction of the superoxide radical ion O_2^- with the active site of Cu, Zn-superoxide dismutase is studied by computer simulation using the ORCA software package version 5.0.2 at the level of density functional theory using the PBE functional and the basis sets of functions def2-SVP, def2-SVPD and def2-TZVPD. The main characteristics for two processes of electron transfer in the catalytic cycle of radical ion deactivation are obtained: reaction potential ΔG^0 , total reorganization energy λ_{tot} , activation energy ΔG^\ddagger , overlap matrix element H_{DA} , and transfer rate constant k according to Marcus. The variable factor in the modeling is the presence of the Zn^{2+} ion at the active site of the enzyme. Two variants of the electron transfer mechanism are considered: one carried out through ligands and another occurring in the immediate vicinity of an oxygen-containing particle and a copper ion. It has been established that the presence of the Zn^{2+} ion contributes to a large extent only to the second electron transfer from the Cu^+ ion to the protonated form of the radical ion, to the hydroperoxide radical HO_2 . Other things being equal, the zinc ion increases the electron transfer rate constant by five times through specific interactions.

Keywords: Cu, Zn-superoxide dismutase, superoxide radical ion, enzyme, reactive oxygen species, antioxidants, condensed state physical chemistry, computer simulation.

Introduction

Molecular oxygen O_2 is an integral part of the energy chains of aerobic organisms. In addition to the benefits that oxygen brings to the body when it is reduced to a water molecule during the redox process, the oxidative power of O_2 can also harm the cellular components of the body. During metabolic transformations, oxygen is able to turn into extremely reactive particles, such as the superoxide radical ion O_2^- considered in this article, the hydroxyl ion OH^- , the hydroxyl radical OH , hydrogen peroxide H_2O_2 , etc. These are the so-called reactive oxygen species (ROS). Their accumulation can adversely affect the state of cell components, destroying them and leading to various diseases of the body as a whole. This phenomenon is called oxidative stress [1, 2].

Antioxidants and antioxidant enzymes provide protection against excessive production of ROS in a healthy body; for example, enzymes of the superoxide dismutase group (SOD) ensure the neutralization of superoxide O_2^- by dismuting it into molecular oxygen and a hydrogen peroxide molecule:



These metalloenzymes include ions of 3d transition elements, such as Cu^{2+} and Zn^{2+} (Cu, Zn-SOD or SOD1), Mn^{3+} (Mn-SOD or SOD2), Fe^{3+} (Fe-SOD), and Ni^{3+} (Ni-SOD) [3, 4].

There are various approximate models for describing the quantum mechanisms of electron transport in condensed states. The model for the case of an electron passing through a one-dimensional static potential barrier over a distance of the order of the barrier width is justified for solid crystalline bodies. This model is not suitable for liquid water-protein media of “living” biochemical systems, where significant relaxation changes occur in the geometry of atoms surrounding the electron transfer channel. Therefore, when conducting this study, we were under the paradigm of the Marcus electron transfer theory for liquid biochemical systems. In this approach, a significant contribution to the value of the potential barrier ΔG^\ddagger is made by the energy of reorganization of the condensed medium and the structure of the nearest environment of the electron transfer channel. In this study, we evaluated all the main characteristics of an effective potential barrier ΔG^\ddagger for transfer between an electron donor and an acceptor. At the same time, the matrix element of the overlapping of the electron molecular orbitals of the donor and acceptor H_{DA} makes it possible to estimate the efficiency of electron tunneling in the semi-quantitative approximation, as a decrease in the height of the classical barrier ΔG^\ddagger due to its quantum “smearing”.

Previously, we studied the stability of the superoxide ion O_2^- [5] in a dielectric medium. Also, using a semi-quantitative technique for such a system as oxygen-SOD1, we evaluated the effect of the properties of a continuous dielectric medium on the primary electron transfer [6]. This technique can be associated with frozen strongly perturbed states during electron transfer. To fully appreciate the electronic and intermolecular effects of interaction in such a system, we apply the opposite but complementary method associated with the Marcus continuum approximation. This is the subject of our consideration in the present study.

This paper considers the main aspects and specifics of the interaction between the superoxide radical ion and the Cu, Zn-SOD active center. The details of the catalytic mechanism are still debatable. Thus, the mechanism of electron transfer is debatable: Does it proceed through the inner-sphere mechanism (in this case, O_2^- comes close enough to the copper ion and acts as a ligand) or through the outer-sphere (in this case, the electron is transferred over a long distance through other ligands associated with the copper ion)? In addition, if the presence of the copper ion Cu^{2+} is necessary for the creation of a redox potential through the formation of a Cu^{2+}/Cu^+ redox pair, then what is the role of the zinc ion Zn^{2+} in the active site? There is evidence that the zinc ion maintains the structure of the site and the Zn-deficient enzyme copes worse with the reduction of O_2^- to H_2O_2 during the secondary electron transfer from Cu^+ , while the secondary transfer becomes pH-dependent [7]. This paper aims to study the processes of electron transfer at two stages of the catalytic process of O_2^- deactivation by enzyme SOD1 and identify the role of the Zn^{2+} ion in this case by comparing the transfer characteristics with “normal” and “Zn-deficient” active sites.

Experimental

Modeling was carried out using the ORCA software package version 5.0.2 [8]. As a calculation method, we applied the level of density functional theory using the GGA density functional of Perdew–Burke–Ernzerhof PBE [9]. The def2-TZVPD basis set [10, 11] was used to optimize the geometry and calculate single point energies of small particles (O_2^- , O_2 , HO_2 , HO_2^- , H_2O , H_3O^+). When optimizing the geometry of the active site, a simplified def2-SVP basis [10] was used with additional restrictions in the form of pinning 8 hydrogen atoms of the methyl end groups to simulate the fact that the active site is retained by the protein environment [12]. After geometry optimization, the one-point energy of the active center structure was calculated with the def2-SVPD basis. In addition, in all cases, when calculating the active center, the oxygen atoms O, copper Cu, and zinc Zn were always subject to the def2-TZVPD basis set. To speed up the hardware calculation, the RI approximation with the basis set def2/J [13] was automatically applied. In any calculation, to consider fine dispersion interactions, the atomic pair dispersion correction algorithm based on rigidly coupled partial charges D4 was used [14, 15]. The influence of the dielectric medium was taken into account using the CPCM continuum model. The surface type is Gaussian VdW [16]. The adequacy of the selection of such calculation parameters was evaluated by one of the important characteristics for molecular oxygen O_2 , which participates in these reactions, namely, by electron affinity in the gas phase. The experimental value $A = -0.451 \pm 0.007$ eV [17]. Our value $A = -0.414$ eV. This approach made it possible to balance the accuracy of the calculation and the cost of hardware time.

To begin with, we should briefly describe the catalytic cycle of the enzyme. Figure 1 shows a simplified process diagram.

The *II–III* and *IV–I* transitions are key to electron transfer. It can be seen that these transitions are complex since the transfer of an electron is coupled with the transfer of a proton H^+ . Since the proton is 1836 times heavier than the electron, the same formalism cannot be applied to it as to the electron. Therefore, the transitions should be divided into more simplified stages in order to be able to describe directly the electron transfer separately from the proton.

It is rather easy to separate transitions *II–III*. Since molecular oxygen O_2 is formed in this case, it is reasonable to assume that the act of electron transfer from O_2^- to the copper ion Cu^{2+} occurs first in a distorted square environment. Then, monovalent copper Cu^+ , which is no longer able to maintain a complex with a coordination number of 4, weakens the bond with the bridging histidine ligand and passes into a trigonal environment, followed by protonation of the nitrogen atom.

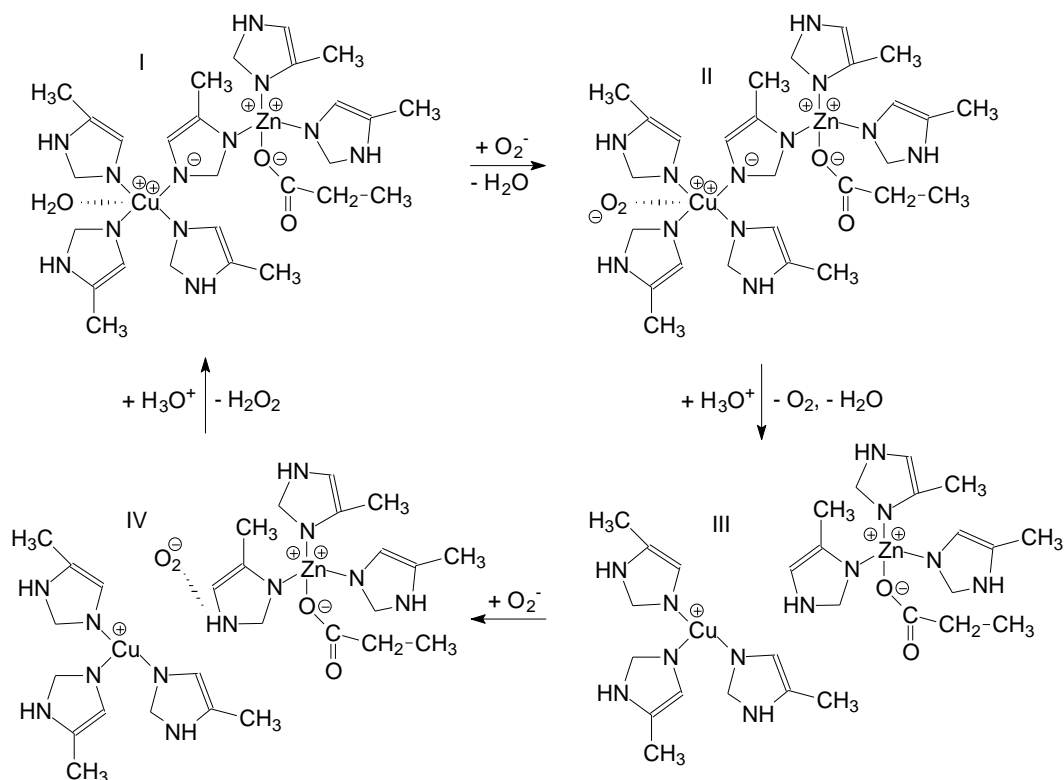


Figure 1. Scheme of the catalytic cycle of dismutation of the superoxide radical ion O_2^- at the active site of copper-zinc superoxide dismutase

IV–I transition is more difficult to separate. This is where the bifurcation occurs. 1. The copper ion Cu^+ in the trigonal environment first donates the electron to the O_2^- ion with the formation of a peroxide ion O_2^{2-} that is not stable in a condensed medium, followed by its protonation to the H_2O_2 molecule. 2. The O_2^- ion accepts a proton from the N–H bond to form the HO_2 hydroperoxide radical, and then the Cu^+ copper ion in the trigonal environment donates the electron to the radical to form the HO_2^- hydroperoxide ion. The simulation showed the predominant flow of process 2, which will be reflected in the results. Figure 2 reflects the above considerations regarding the choice of stages for electron transfer.

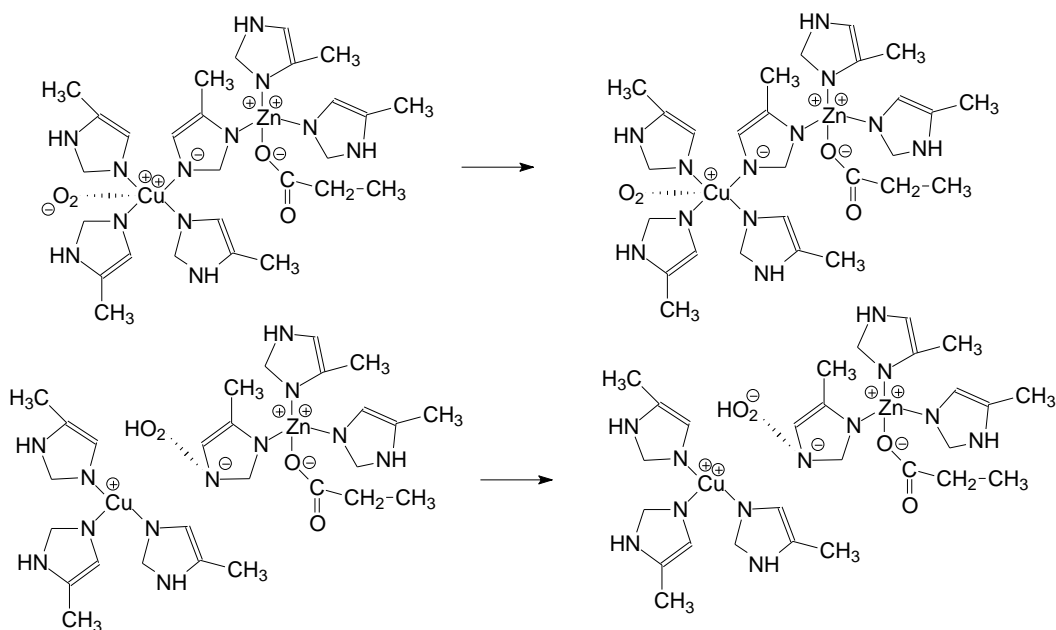


Figure 2. Separately distinguished stages of primary and secondary electron transfers

Besides, for the case of a Zn-deficient active site, the Zn^{2+} ion was removed from the structure of the active site and replaced by two equivalent H^+ protons. The first of them was attached to the oxygen atom of the former zinc ligand, and the second, to the nitrogen atom of the former bridging ligand. Figure 3 presents the scheme for the removal of zinc ion.

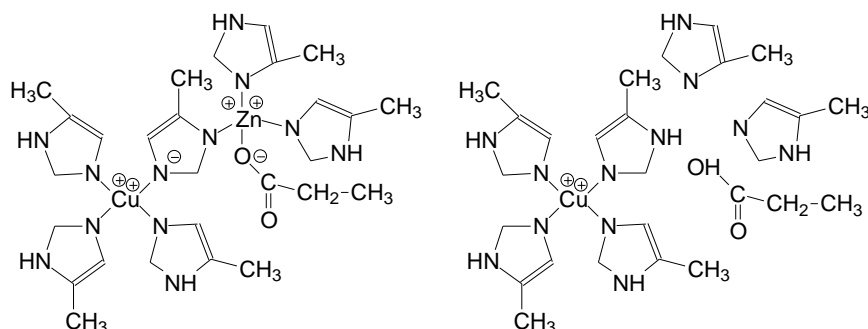


Figure 3. Scheme for the removal of zinc ion from the active site

The efficiency of electron transfer can be estimated to a complete extent by obtaining the value of the second-order transfer rate constant k (hereinafter, we denote I as primary transfer and II as secondary):



$$\frac{dC}{dt} = -k_I \cdot [O_2^-] \cdot [Cu^{2+}]; \quad (2)$$



$$\frac{dC}{dt} = -k_{II} \cdot [HO_2^-] \cdot [Cu^+]. \quad (4)$$

In general, the rate constant k for reactions (1) and (3) can be estimated using an analogue of the Eyring equation for the activated complex theory [18]:

$$k = k_{et} \cdot K_{pre}^\ddagger, \quad (5)$$

where k_{et} — the frequency factor of electron transfer according to Marcus, s-1; K_{pre}^\ddagger — the concentration equilibrium constant of the formation of the precursor complex from the electron donor and acceptor, M-1.

The frequency factor k_{et} or the first-order rate constant of electron transfer can be calculated using the Marcus formalism [19]:

$$k_{et} = \frac{4 \cdot \pi^2}{h} \cdot \frac{H_{DA}^2}{\sqrt{4 \cdot \pi \cdot \lambda_{tot} \cdot k_B \cdot T}} \cdot e^{\frac{-\Delta G^\ddagger}{k_B \cdot T}}. \quad (6)$$

where h — the Planck's constant, J·s; H_{DA} — the matrix element of overlapping molecular orbitals of the electron donor and acceptor, J; λ_{tot} — the total energy of the system reorganization, J; k_B — the Boltzmann constant; J/K; T — temperature, K; ΔG^\ddagger — the transfer activation energy, J.

a. Calculation of the reaction potential ΔG^0

According to the Hess law and the principle of the quantum dimension of the system, the change in the potential of the electron transfer reaction was calculated according to the scheme:

$$\Delta G_I^0 = G^0(O_2) + G^0(ICu^+SOD) - G^0(O_2^-) - G^0(ICu^{2+}SOD); \quad (7)$$

$$\Delta G_{II}^0 = G^0(HO_2^-) + G^0(IICu^{2+}SOD) - G^0(HO_2) - G^0(IICu^+SOD). \quad (8)$$

It is also necessary to calculate the “corrected” value of ΔG^{0*} — adjusted for the fact that the electron transfer occurs not at infinity, but at a specific finite distance R . To do this, we use the expression proposed in [20]:

$$\Delta G^{0*} = \Delta G^0 + (Z_A - Z_D - 1) \cdot \frac{1}{4 \cdot \pi \cdot \epsilon_0} \cdot \frac{q_e^2}{\epsilon \cdot R}. \quad (9)$$

where Z_A — the charge number of the acceptor; Z_D — the charge number of the donor; ϵ_0 — the electrical constant, F/m; q_e — the electron charge, C; R — the transfer distance, m; ϵ — the static permittivity of the medium.

The transfer distance R is an extremely ambiguous value and can vary greatly. The principle of choosing R values is presented below.

b. Calculation of the total reorganization energy λ_{tot}

The reorganization energy is the energy that must be expended to bring the system into a state as if the electron transfer had already occurred, but *de facto* without it. The total reorganization energy consists of two components. The first one is the internal λ_{in} , which includes the energy spent on rearranging the structure of the donor and acceptor for electron transfer. The second is the external λ_{out} , which includes the energy consumption for the rearrangement of the structure of the environment surrounding the donor and acceptor, the solvent.

The calculation of λ_{in} is generally similar to the calculation of the reaction potential, but with a difference in the products. Here it is necessary to take perturbed structures as finite particles, for example, if in its ground state the superoxide ion O_2^- has, according to our modeling, an equilibrium internuclear distance of 1.353 Å in the charge state -1 , then the perturbed structure corresponding to it will have an internuclear distance of 1.218 Å (as in molecular oxygen O_2) in the charge state -1 . Single point energy without optimization of the geometry of such structures is denoted by *.

$$\lambda_{\text{in}}^I = G^{0*}(\text{O}_2^-) + G^{0*}(\text{ICu}^{2+}\text{SOD}) - G^0(\text{O}_2^-) - G^0(\text{ICu}^{2+}\text{SOD}); \quad (10)$$

$$\lambda_{\text{in}}^{II} = G^{0*}(\text{HO}_2) + G^{0*}(\text{IICu}^+\text{SOD}) - G^0(\text{HO}_2) - G^0(\text{IICu}^+\text{SOD}). \quad (11)$$

Markus and Sutin proposed the calculation of λ_{out} in the approximation of the solvent continuum model [19]:

$$\lambda_{\text{out}} = \frac{\Delta q^2}{4 \cdot \pi \cdot \epsilon_0} \cdot \left(\frac{1}{2r_D} + \frac{1}{2r_A} - \frac{1}{R} \right) \cdot \left(\frac{1}{n^2} - \frac{1}{\epsilon} \right), \quad (12)$$

where Δq — the value of the transferred charge, C; r_D — the donor radius, m; r_A — the acceptor radius, m; n — the refractive index of the medium.

The size of the transfer participants was estimated from the following considerations. All reagents were presented as spheres with certain radii r . Thus, the radius of the superoxide ion O_2^- was calculated as the sum of the radius of the oxygen atom according to the continuum model (this is 1.52 Å) and half the length of the O–O bond (this is 0.6765 Å from 1.353 Å). In the case of such a small particle, a solvent correction is also needed [20]. When using the continuum model, it makes sense to add half of the probe radius (this is 0.65 Å from 1.3 Å). We have the radius of the donor sphere centered in the middle of the bond $r_{DII}(\text{O}_2^-) = 2.8465$ Å. By using a similar approach, we can obtain $r_{AII}(\text{HO}_2) = 2.8365$ Å for the HO_2 acceptor. Also, for the active site, it is logical to choose only such a region that changes significantly during the redox process. This is the first ligand environment of the copper ion. A sphere centered on a copper ion with an average radius extending to the second nitrogen atom in the imidazole ring of the ligands was chosen with the addition of the radius of the nitrogen atom according to the continuum model of 1.89 Å. We have $r_{AII}(\text{Cu}^{2+}\text{SOD}) = 6.035$ Å. By analogy, for the monovalent copper state, one can obtain $r_{DII}(\text{Cu}^+\text{SOD}) = 6.040$ Å. For the Zn-deficient active site, the corresponding values are 6.047 Å and 6.034 Å.

To estimate the transfer rate constant by the outer-sphere mechanism, two reference values of R can be chosen. The first of them is the sum of the donor and acceptor radii. In our case, this is 8.88 Å. The second value is 6 Å, chosen from the consideration that a positively charged aspartic group adjoins the active center at this distance, which is capable of directing O_2^- to the reaction. Also, for the inner-sphere mechanism, the distance R is determined, for the most part, by optimizing the O_2^- geometry in close proximity to the copper ion.

c. Calculation of the transfer activation energy ΔG^\ddagger

Knowing the values of the reaction potential ΔG^{0*} and λ_{tot} , it is possible to determine the value of the activation energy [20] according to the equation:

$$\Delta G^\ddagger = \frac{1}{4 \cdot \pi \cdot \epsilon_0} \cdot \frac{Z_D \cdot Z_A \cdot q_e^2}{\epsilon \cdot R} + \frac{1}{4} \cdot \lambda_{\text{tot}} \cdot \left(1 + \left(\frac{\Delta G^{0*}}{\lambda_{\text{tot}}} \right)^2 \right). \quad (13)$$

d. Calculation of the overlap matrix element H_{DA}

The overlapping matrix element of the molecular orbitals of the electron donor and acceptor can be estimated using the generalized Mulliken–Hush (GMH) approximation [21]:

$$H_{DA} = \frac{\Delta E_{12} \cdot \mu_{12}}{\sqrt{\Delta \mu_{12}^2 + 4 \cdot \mu_{12}^2}}, \quad (14)$$

where ΔE_{12} — the energy of electron transition from the MO of the donor to the MO of the acceptor, J; μ_{12} — the transition dipole moment, C·m; $\Delta \mu_{12}$ — the difference between dipole moments before and after electron transfer, C·m.

The values included in (14) were estimated using the time-dependent density functional theory (TD-DFT) using the default TDA approximation.

e. Calculation of the equilibrium constant for the formation of the precursor complex K_{pre}^\ddagger

The equilibrium constant K_{pre}^\ddagger can be obtained based on various considerations. We used one of the expressions presented in [18], in which it suffices to know the work of approach of the donor and acceptor W_R and the electron transfer distance R :

$$K_{pre}^\ddagger = \frac{4}{3} \cdot \pi \cdot N_A \cdot R^3 \cdot e^{\frac{-W_R}{k_B \cdot T}}, \quad (15)$$

where N_A — the Avogadro constant, mol⁻¹; R — the transfer distance, dm; W_R — the electrostatic work of bringing the reagents together at a distance R , J.

$$W_R = \frac{1}{4 \cdot \pi \cdot \epsilon_0} \cdot \frac{Z_D \cdot Z_A \cdot q_e^2}{\epsilon \cdot R}. \quad (16)$$

Here and below, when calculating according to the above expressions, the temperature value T is equal to the standard 298.15 K.

Results and Discussion

To begin with, we point out that the experimental values of k for both primary and secondary electron transfers do not depend on the charge of the copper ion and are equal to $2 \cdot 10^9$ M⁻¹·s⁻¹ [22].

Thus, let us consider the main characteristics of the primary electron transfer of the **II–III** transition between the superoxide radical ion O₂⁻ and the copper ion Cu²⁺ according to the outer-sphere mechanism at a distance of 6 Å perpendicular to the square environment of copper (Table 1).

Table 1

Characteristics of primary electron transfer at $R = 6$ Å

Parameter	SOD1	Zn-deficient SOD1
ΔG^0 , eV	-0.444	-0.491
ΔG^{0^*} , eV	-0.385	-0.431
λ_{tot} , eV	1.754	1.686
ΔG^\ddagger , eV	0.208	0.174
H_{DA} , eV	$1.68 \cdot 10^{-2}$	$2.51 \cdot 10^{-3}$
k_{et} , s ⁻¹	$1.11 \cdot 10^9$	$9.37 \cdot 10^7$
K_{pre}^\ddagger , M ⁻¹	5.56	5.56
k , M ⁻¹ ·s ⁻¹	$6.15 \cdot 10^9$	$5.21 \cdot 10^8$

Similar values of the rate constants of electron transfer at the same distance with and without zinc ion indicate that the zinc ion does not play an important role in the first stage of deactivation of the superoxide ion.

It should be noted that the overlap of the donor and acceptor molecular orbitals decays with increasing transfer distance. Since the overlap matrix element, along with the activation energy, makes the most significant contribution to the rate constant, we can compare how the matrix element decays with the transfer distance for the active site with and without zinc ion. The dependence of the overlap matrix element was assumed to be exponential [23]:

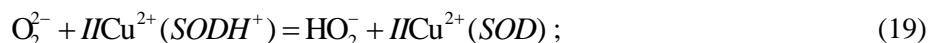
$$H_{DA} = H_{DA}^0 \cdot e^{-\alpha \cdot (R - R_0)}, \quad (17)$$

where H_{DA}^0 — the value of the matrix element at the distance $R_0 = r_D + r_A$; α — the overlap damping constant, Å⁻¹.

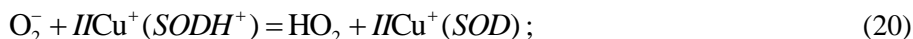
We obtained the following correlation equations for SOD1 $\alpha = 1.173$ Å⁻¹ and Zn-deficient SOD1 $\alpha = 0.573$ Å⁻¹. For SOD1, the overlap integrals of molecular orbitals decay 2 times faster than for zinc-

deficient. However, such a value is not particularly critical, given the similar values of the rate constants we obtained.

Next, we consider the main characteristics of the secondary electron transfer of the *IV–I* transition between the hydroperoxide radical HO₂ and the copper ion Cu⁺ according to the outer-sphere mechanism at a distance of 6 Å. Let us give an explanation regarding the bifurcation discussed above. Why was HO₂ chosen as the electron acceptor, and not O₂⁻? Does this mean that the proton transfer occurs before the electron transfer? It is necessary to study the potentials of the corresponding reactions to answer this question:



$\Delta G_{20}^0 = +2.84$ eV. $\Delta G_{21}^0 = -1.90$ eV. Sum: 0.94 eV.



$\Delta G_{22}^0 = +0.354$ eV. $\Delta G_{23}^0 = -0.39$ eV. Sum: -0.036 eV.

It is natural to choose scheme 2 (20–21) as the model scheme for secondary transfer. Further, it should be pointed out that the superoxide ion O₂⁻ is no longer bound by the copper ion Cu⁺ in the trigonal environment that is stable for such a valence state, but elsewhere. According to the geometry optimization results, O₂⁻ tends to the source of protons, in this case, to the N–H bond of the bridging ligand. This proton is split off from the nitrogen atom and goes to the radical.

Table 2

Characteristics of secondary electron transfer at R = 6 Å

Parameter	SOD1	Zn-deficient SOD1
ΔG^0 , eV	-0.390	-0.044
ΔG^{0*} , eV	-0.449	-0.104
λ_{tot} , eV	1.603	1.672
ΔG^\ddagger , eV	0.208	0.368
H_{DA} , eV	$1.91 \cdot 10^{-1}$	$3.70 \cdot 10^{-2}$
k_{ets} , s ⁻¹	$1.49 \cdot 10^{11}$	$1.08 \cdot 10^7$
K_{pre^\ddagger} , M ⁻¹	0.545	0.545
k , M ⁻¹ ·s ⁻¹	$8.12 \cdot 10^{10}$	$5.86 \cdot 10^6$

As can be seen, the effects mainly concern only the secondary electron transfer. This indicates that the copper ion Cu⁺ in the absence of Zn²⁺ becomes less labile with respect to the loss of an electron with the formation of Cu²⁺. The effect is on all quantities that determine the value of the rate constant. Significant differences in the rate constants, both of the first order and of the second order, indicate that zinc-deficient SOD1 copes much worse with the role of a catalyst. The frequency transfer factor in this case is less by five orders of magnitude than for the “normal” SOD1.

The removal of the zinc ion increases the value of the isobaric-isothermal transfer potential ΔG^0 by 0.35 eV. Let's write its value as:

$$\Delta G^0 = z \cdot F \cdot \left(E^0 \left(\text{SOD}^{2+} / \text{SOD}^+ \right) - E^0 \left(\text{HO}_2 / \text{HO}_2^- \right) \right) \quad (22)$$

where z — the number of transferred electrons; F — the Faraday constant, C/mol; E^0 — the standard electrode potential, V.

It can be seen that the value of the standard electrode potential of the SOD active center increases. The oxidizing properties of the center are enhanced and the reducing properties are weakened. The oxidizing properties of the center are weakened and the reducing properties are enhanced. The reorganization energy somewhat increases by 0.07 eV due to the structural component. The zinc ion in a tetrahedral environment more stabilizes the system and limits the geometric transformations of the active center after electron transfer. Thus, with a change in these parameters, the activation energy of the second transfer for the Zn-deficient center increases by about 16 kJ/mol. Given that the rate constant has a quadratic dependence on H_{DA} , this effect is more significant than the increase in the transfer activation energy.

There is clear participation of the bridging histidine ligand in the formation of the donor MO of the active site, which promotes electron transfer. When the zinc ion is removed, the ligand is no longer bridging and becomes more independent, while it does not take part in the formation of the donor MO.

As for the primary transfer, let us analyze the attenuation coefficient of the orbital overlap for the secondary transfer. For SOD1 $\alpha = 0.047 \text{ \AA}^{-1}$ and Zn-deficient SOD1 $\alpha = 0.569 \text{ \AA}^{-1}$. Here, we observe a significant difference in the values of the indicator. The extremely low value for SOD1 indicates that the attenuation of the orbital overlap is extremely weak and can reach significant values for the implementation of electron transfer, even at large distances through ligands. The obtained molecular orbitals for SOD1 and zinc-deficient SOD1 for secondary transfer show that the bridging ligand connecting copper and zinc ions is also involved in the formation of the outer orbital. This indicates the low attenuation and the participation of ligands in the transfer.

It is reasonable to trace the distribution of an atomic-molecular characteristic, such as atomic charge, throughout the active center before and after electron transfer. Let us look at the changes in atomic charges according to Löwdin during the transition from IICu^+SOD to $\text{IICu}^{2+}\text{SOD}$ with secondary (II) electron transfer:

- “normal” SOD1: $\Delta_q\text{Cu} = +0.177$; $\Delta_q\text{Zn} = +0.008$. The contribution of zinc is 4.3 %.
- Zn-deficient SOD1: $\Delta_q\text{Cu} = +0.188$.

The difference between the atomic charges according to Löwdin for the copper atom Cu in IICu^+SOD with and without the zinc ion Zn^{2+} is $\Delta_q\text{Cu} = {}_q\text{Cu} - {}_q\text{Cu}(\text{Zn}) = +0.021$ (increase by 45 %). Based on the above results on the population, we can conclude that, in addition to the structural organization of the active site, the zinc ion Zn^{2+} contributes to the partial delocalization of the electron density, accepting part of it through the ligand bridge together with the copper ion Cu^+ .

Let us now look at the changes in atomic charges according to Löwdin during the transition from $\text{ICu}^{2+}\text{SOD}$ to ICu^+SOD during the primary (I) electron transfer.

- “normal” SOD1: $\Delta_q\text{Cu} = -0.314$; $\Delta_q\text{Zn} = -0.007$. The contribution of zinc is 2.2 %.
- Zn-deficient SOD1: $\Delta_q\text{Cu} = -0.321$.

The difference between atomic charges according to Löwdin for copper atom Cu in ICu^+SOD with and without zinc ion Zn^{2+} is $\Delta_q\text{Cu} = {}_q\text{Cu} - {}_q\text{Cu}(\text{Zn}) = 0.0006$. This implies another proof of the fact that the zinc ion Zn^{2+} has a much greater influence only on the secondary electron transfer.

It has been experimentally established that the reaction catalyzed by Zn-deficient superoxide dismutase becomes pH-dependent on secondary electron transfer [7]. We present the calculated values of ΔG^0 for the processes of O_2^- protonation from the N–H bond before the secondary electron transfer in SOD1 and Zn-deficient SOD1: +0.354 eV and +0.712 eV, respectively. In the absence of zinc, the cost of protonation doubles, which indicates the stabilization of the protonated form of the histidine ligand, which is free of both the zinc ion Zn^{2+} and the copper ion Cu^+ . Such an increase in energy creates certain difficulties for the preliminary formation of HO_2 ; therefore, the presence of an external proton from the solvent molecules is required. For example, its source can be the hydronium ion H_3O^+ . This explains why the removal of zinc results in a pH-dependent electron transfer.

Conclusions

All two-electron transfer processes are associated with proton transfer. The primary electron transfer occurs somewhat earlier than the proton transfer. In the case of secondary transfer, the situation is reversed. A proton from the N–H bond of the bridging ligand is able to attach to the superoxide ion to form HO_2 , which then readily accepts an electron. The zinc ion Zn^{2+} has little effect on the primary electron transfer from O_2^- to the copper ion Cu^{2+} . Its presence in the active site creates a suitable conformation for efficient overlapping of the donor and acceptor MOs and creates an additional minor electron density delocalization. At the same time, the zinc ion Zn^{2+} has a significant effect on the secondary electron transfer from Cu^+ to HO_2 . When the zinc ion is removed, the transfer rate constant decreases by five times. This is due to a significant positive increase in the value of the transfer reaction potential, which in turn increases the activation energy. Thus, the zinc ion, by its presence in the active center, stabilizes the structure in such a way that during the secondary electron transfer from the active center, its redox potential increases and the reduction properties decrease. According to the results obtained, it follows that the redox potential increases by 0.35 V. The bridging ligand retained by the zinc ion is able to participate in the formation of orbital overlap during transfer, in contrast to the case of zinc removal. The participation of the ligand reduces the degree of damping of the overlap integrals and promotes rapid electron transfer. In addition, the electron density distribution

between copper and zinc ions makes it easier for the proton to break away from the ligand and then attach to the oxygen-containing particle.

References

- 1 Barja, G. (1999). Mitochondrial Oxygen Radical Generation and Leak: Sites of Production in States 4 and 3, Organ Specificity, and Relation to Aging and Longevity. *J. Bioenergetics and Biomembranes*, 31, 347–366. <https://doi.org/10.1023/A:1005427919188>
- 2 Dawson, T.M., & Dawson, V.L. (2003). Molecular Pathways of Neurodegeneration in Parkinson's Disease. *Science*, 302, 5646. <https://doi.org/10.1016/B978-0-323-88460-0.00010-2>
- 3 Fridovich, I. (1997). Superoxide anion radical (O_2^-), superoxide dismutase and related matters. *J. Biol. Chem.*, 272, 18515–18517. <https://doi.org/10.1074/jbc.272.30.18515>
- 4 Cabelli, D.E., Riley, D., Rodriguez, J.A., Valentine, J.S., & Zhu, H. (1999). *Models of superoxide dismutases. Biomimetic Oxidations Catalyzed by Transition Metal Complexes*. Imperial College Press, 461–508. https://doi.org/10.1142/9781848160699_0010
- 5 Ryabykh, A.V., Maslova, O.A., Beznosyuk, S.A., Zhukovsky, M.S., & Masalimov, A.S. (2020). Computer Simulation of the O_2^- Superoxide Ion Stability in a Continuous Dielectric Medium. *Izvestiya of Altai State University*, 1(111), 36–40. [https://doi.org/10.14258/izvasu\(2020\)1-05](https://doi.org/10.14258/izvasu(2020)1-05)
- 6 Maslova, O.A., Ryabykh, A.V., & Beznosyuk, S.A. (2020). Computer simulation of SOD interaction with reactive oxygen species in low-sized membrane cell nanostructures. *AIP Conference Proceedings*, 2310, 020196. <https://doi.org/10.1063/5.0034337>
- 7 Ellerby, L.M., Cabelli, D.E., Graden, J.A., & Valentine, J.S. (1996). Copper-Zinc Superoxide dismutase: Why Not pH-Dependent. *J. Am. Chem. Soc.*, 118, 6556–6561. <https://doi.org/10.1021/ja953845x>
- 8 Neese, F. (2012). The ORCA program system. *Wiley interdisciplinary Reviews — Computational Molecular Science*, 2(1), 73–78. <https://doi.org/10.1002/wcms.81>
- 9 Perdew, J.P., Burke, K., & Ernzerhof, M. (1996). Generalized Gradient Approximation Made Simple. *Phys. Rev. Letters*, 77, 3865. <https://doi.org/10.1103/physrevlett.77.3865>
- 10 Weigend, F. & Ahlrichs, R. (2005). Balanced basis sets of split valence, triple zeta valence and quadruple zeta valence quality for H to Rn: Design and assessment of accuracy. *Phys. Chem. Chem. Phys.*, 7, 3297. <https://doi.org/10.1039/b508541a>
- 11 Rappoport, D. & Furche, F. (2010). Property-optimized Gaussian basis sets for molecular response calculations. *J. Chem. Phys.*, 133, 134105. <https://doi.org/10.1063/1.3484283>
- 12 Xerri, B., Petitjean, H., Dupeyrat, F., Flament, J.-P., Lorphelin, A., Vidaud, C., et al. (2014). Mid- and Far-Infrared Marker Bands of the Metal Coordination Sites of the Histidine Side Chains in the Protein Cu, Zn-Superoxide Dismutase. *European Journal of Inorganic Chemistry*, 2014(27), 4650–4659. <https://doi.org/10.1002/ejic.201402263>
- 13 Weigend, F. (2006). Accurate Coulomb-fitting basis sets for H to Rn. *Phys. Chem. Chem. Phys.*, 8, 1057. <https://doi.org/10.1039/b515623h>
- 14 Grimme S., Antony, J., Ehrlich, S. & Krieg, H. (2010). A consistent and accurate ab initio parametrization of density functional dispersion correction (DFT-D) for the 94 elements H-Pu. *J. Chem. Phys.*, 132, 154104. <https://doi.org/10.1063/1.3382344>
- 15 Caldeweyher, E., Bannwarth, C. & Grimme, S. (2017). Extension of the D3 dispersion coefficient model. *J. Chem. Phys.*, 147, 034112. <https://doi.org/10.1063/1.4993215>
- 16 Cossi, M., Rega, N. & Scalmani, G. et al. (2003). Energies, structures and electronic properties of molecules in solution with the C-PCM solvation model. *Chem. Phys.*, 24, 669–681. <https://doi.org/10.1002/jcc.10189>
- 17 Rienstra-Kiracofe, J.C., Tschumper, G.S., & Shaefer, H.F. (2002). Atomic and molecular electron affinities: photoelectron experiments and theoretical computations. *Chem. Rev.*, 102, 231–282. <https://doi.org/10.1021/cr990044u>
- 18 Lippard, S.J. (1978). Theory of Electron Transfer Reactions: Insights and Hindsight. *Progress in Inorganic Chemistry*, 30, 441–498. <https://doi.org/10.1002/9780470166314.ch9>
- 19 Marcus, R.A., & Sutin, N. (1985). Electron transfers in chemistry and biology. *Biochimica et Biophysica Acta*, 811, 265–322. [https://doi.org/10.1016/0304-4173\(85\)90014-x](https://doi.org/10.1016/0304-4173(85)90014-x)
- 20 Ebersson, L. (1985). The Marcus theory of electron transfer, a sorting device for toxic compounds. *Advances in Free Radical Biology & Medicine*, 1, 19–90. [https://doi.org/10.1016/8755-9668\(85\)90004-3](https://doi.org/10.1016/8755-9668(85)90004-3)
- 21 Cave, R.J., & Newton, M.D. (1997). Calculation of electronic coupling matrix elements for ground and excited state electron transfer reactions: Comparison of the generalized Mulliken-Hush and block diagonalization methods. *Journal of Chemical Physics*, 106, 9213–9226. <https://doi.org/10.1063/1.474023>
- 22 Takahashi, M.A., & Asada, K. (1982). A flash-photometric method for determination of reactivity of superoxide: application to superoxide dismutase assay. *Journal of biochemistry*, 91(3), 889–896. <https://doi.org/10.1093/oxfordjournals.jbchem.a133777>
- 23 Hopfield, J.J. (1974). Electron transfer between biological molecules by thermally activated tunneling. *Proceedings of the National Academy of Sciences of the United States of America*, 71(9), 3640–3644. <https://doi.org/10.1073/pnas.71.9.3640>

A.В. Рябых, О.А. Маслова, С.А. Безносюк, А.С. Масалимов

Мыс-мырыш супероксид дисмутазасының белсенді орталығындағы мырыш ионының рөлі

PBE функционалын және def2-SVP, def2-SVPD мен def2-TZVPD функцияларының базистік жиынтықтарын пайдалана отырып, тығыздық функционалы теориясының деңгейінде ORCA 5.0.2 нұсқасының бағдарламалық пакетінің көмегімен компьютерлік модельдеу арқылы O_2^- супероксидті ион-радикалының Cu, Zn-супероксиддисмутазаының белсенді орталығымен өзара әрекеттесуіне зерттеу жүргізілді. Ион-радикалды дезактивациялаудың каталитикалық цикліндегі электрон тасымалдаудың екі процесінің негізгі сипаттамалары алынған: ΔG^0 реакция потенциалы, λ_{tot} жалпы қайта құру энергиясы, ΔG^\ddagger активтену энергиясы, H_{DA} қабаттасатын матрица элементі және Маркус бойынша k тасымалдау жылдамдығының тұрақтысы. Модельдеу барысындағы өзгермелі фактор ретінде ферменттің белсенді орнында Zn^{2+} ионының орналасуы алынды. Лигандтардың көмегімен және құрамында оттегі бар бөлшек пен мыс ионының жақын орналасуы арқылы жүзеге асырылатын электронды тасымалдау механизмінің екі нұсқасы қарастырылды. Zn^{2+} ионының болуы тек Cu^+ ионынан ион-радикалының протондалған формасына — HO_2 гидропероксид радикалына екінші электронның өтуіне ғана үлкен дәрежеде ықпал ететіні анықталды. Арнайы өзара әрекеттесулер арқылы мырыш ионы, басқа жағдайлар бірдей болғанда электронды тасымалдау жылдамдығының константасын бес реттік шамаға арттырады.

Кілт сөздер: Cu, Zn-супероксиддисмутаза, супероксидті ион-радикал, фермент, реактивті оттегі түрлері, антиоксиданттар, конденсацияланған күйдің физика-химиясы, компьютерлік модельдеу.

A.В. Рябых, О.А. Маслова, С.А. Безносюк, А.С. Масалимов

Роль иона цинка в активном центре медно-цинковой супероксиддисмутазы

Проведено изучение взаимодействия супероксидного ион-радикала O_2^- с активным центром Cu, Zn-супероксиддисмутазы путем компьютерного моделирования при помощи программного пакета ORCA версии 5.0.2 на уровне теории функционала плотности с использованием функционала PBE и базисных наборов функций def2-SVP, def2-SVPD и def2-TZVPD. Получены основные характеристики для двух процессов переноса электрона в каталитическом цикле дезактивации ион-радикала: потенциал реакции ΔG^0 , полная энергия реорганизации λ_{tot} , энергия активации ΔG^\ddagger , матричный элемент перекрытия H_{DA} и константа скорости переноса k по Маркусу. Переменным фактором при моделировании являлось наличие иона Zn^{2+} в активном центре фермента. Были рассмотрены два варианта механизма переноса электрона, осуществляющихся при помощи лигандов и непосредственной близости кислородсодержащей частицы и иона меди. Установлено, что наличие иона Zn^{2+} способствует в значительной степени только второму переносу электрона от иона Cu^+ к протонированной форме ион-радикала — к гидропероксидному радикалу HO_2 . Посредством специфических взаимодействий ион цинка при прочих равных условиях повышает константу скорости переноса электрона на пять порядков.

Ключевые слова: Cu, Zn-супероксиддисмутаза, супероксидный ион-радикал, фермент, активные формы кислорода, антиоксиданты, физикохимия конденсированного состояния, компьютерное моделирование.

Information about authors*

Ryabikh, Andrey Valerievich — Assistant and Engineer, Department of Physical and Inorganic Chemistry, Altai State University, Barnaul, Lenina avenue, 61; e-mail: ryabikh@chem.asu.ru; <https://orcid.org/0000-0003-3699-3932>;

Maslova, Olga Andreevna — Candidate of Physical and Mathematical Sciences, Associate Professor, Physical and Inorganic Chemistry Department, Altai State University, Barnaul, Lenina avenue, 61; e-mail: maslova_o.a@mail.ru; <https://orcid.org/0000-0003-3862-3687>;

Beznosyuk, Sergey Alexandrovich (corresponding author) — Doctor of Physical and Mathematical Sciences, Professor, Head of the Physical and Inorganic Chemistry Department, Altai State University, Barnaul, Lenina avenue, 61; e-mail: bsa1953@mail.ru; <https://orcid.org/0000-0002-4945-7197>;

Masalimov, Abay Sabirzhanovich — Full Professor, Doctor of Chemical Sciences, Physical and Analytical Chemistry Department, Karagandy University of the name of academician E.A. Buketov, Universitetskaya street, 28, 100024, Karaganda, Kazakhstan; e-mail: masalimov-as@mail.ru; <https://orcid.org/0000-0002-6405-7108>

*The author's name is presented in the order: Last Name, First and Middle Names